

微合金化铸铁同质焊条焊接工艺

翟秋亚， 翟 波， 唐 桢， 徐锦锋
(西安理工大学 材料科学与工程学院, 西安 710048)

摘 要: 应用微合金化铸铁同质焊条, 采用小电流打底、大电流连续焊工艺, 研究了预热温度与焊缝组织及性能之间的相关性。结果表明, 微合金化铸铁焊条石墨化能力强, 焊缝白口倾向小; 小电流打底、大电流连续焊工艺可有效地减小熔深, 在很大程度上抑制了熔合区白口的产生。微合金化铸铁焊条可实现常温焊接。预热温度小于 200℃即可获得组织和性能与母材一致的同质焊缝。随着焊件预热温度的升高, 焊缝中的石墨形态由细小的点状逐渐向菊花状、片状过渡, 铁素体含量增多, 焊缝硬度减小。焊件预热至 200℃所获得的焊缝组织由珠光体、铁素体和细片状石墨及菊花状石墨组成, 熔合区则由珠光体、少量碎块状铁素体及过冷石墨片组成, 接头力学性能良好。

关键词: 微合金化铸铁焊条; 铸铁件; 常温焊; 接头组织与性能

中图分类号: TG143 文献标识码: A 文章编号: 0253-360X(2007)10-053-04



翟秋亚

0 序 言

由于铸造工艺的复杂性, 铸铁件在生产过程中不可避免的会产生各种铸造缺陷, 如气孔、夹渣、缩孔、缩松和裂纹等。据统计, 中国目前年产铸铁件已突破 800 万吨^[1], 不良品率平均约 10%~15%。因此, 对缺陷铸铁件进行焊接修复具有重大的经济意义。但是, 由于铸铁的焊接性差^[2], 焊接过程中焊补区极易产生渗碳体、马氏体和贝氏体等淬硬组织, 严重影响焊接接头的力学性能。应用多元微合金化铸铁同质焊条可在铸件不预热或低的预热温度下获得与母材组织和性能一致的焊接接头^[3,4]。然而, 有关焊接工艺对微合金化铸铁同质焊条焊接接头组织和性能影响规律的研究相对较少。文中采用自行研制的微合金化铸铁同质焊条对灰铁板材进行焊接工艺研究, 探索焊接工艺与接头组织和性能的相关规律, 为铸铁件的焊接提供理论依据。

1 试 验

1.1 试验材料

1.1.1 焊条的制备

微合金化铸铁焊芯用自有专利技术——真空吸

收稿日期: 2007-06-18
基金项目: 陕西省教育厅科学研究计划资助项目(07JK351); 西安市科技攻关计划资助项目(GG06069); 2006 年西安市青年科技人才创业计划资助项目

铸法制备而成。采用 25 kg 中频感应炉熔配铁液。焊芯目标化学成分见表 1。焊芯规格为 $\phi 5\text{ mm}\times 400\text{ mm}$ 。用 JHY-25 型液压涂粉机外涂碱性石墨化型药皮。

表 1 焊芯目标化学成分(质量分数, %)
Table 1 Chemical composition of electrode core

C	Si	Mn	P	S	Ca	Ni	Ti	Bi	Fe
3.6~4.0	3.6~4.6	≤0.5	≤0.1	≤0.05	1.0	0.8	0.8	0.02	余量

1.1.2 焊件的准备

参照机床床身材质和壁厚, 焊件材质选取 HT250, 焊件尺寸为 1 000 mm×200 mm×35 mm。在焊件的上表面加工出 V 形坡口, 如图 1 所示。

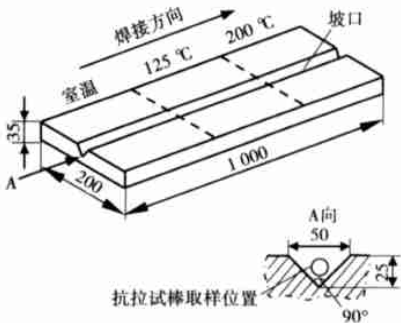


图 1 焊件结构与尺寸及取样位置(mm)
Fig 1 Structure and size of welding piece and sampling location

1.2 试验方法

使用直流焊机反接极施焊,对自行研制的微合金化铸铁同质焊条进行焊接工艺研究。采用小电流($I=150\sim180\text{ A}$)打底,大电流($I=250\sim280\text{ A}$)连续焊工艺。焊件预热温度 T_0 分别取 $0\text{ }^{\circ}\text{C}$ (室温)、 $125\text{ }^{\circ}\text{C}$ 和 $200\text{ }^{\circ}\text{C}$ 三种。用 MCT-100 电脑化精密数字测温仪检测焊件表面温度。

沿焊缝横截面方向截取焊接接头金相试样。用光学显微镜观察接头的组织形态。用体视学原理定量分析物相的体积分数。用光谱仪分析焊缝金属的化学成分。并用硬度仪测定接头各区的硬度。沿焊缝长度方向制取 $\phi 10\text{ mm}$ 的熔敷金属单肩拉伸试棒,在万能试验机上测定焊缝金属的抗拉强度。

2 结果与讨论

2.1 焊接接头组织特征

图 2 为焊件预热到 $200\text{ }^{\circ}\text{C}$ 时焊接接头的整体形貌。从图中可以看出,焊接接头由焊缝、熔合区和热影响区组成。熔合区宽度约 $245\text{ }\mu\text{m}$,焊缝与母材结合良好。热影响区组织由珠光体、少量铁素体和粗片状石墨组成。焊缝组织由珠光体、铁素体和细片状石墨组成。焊缝中白色区域较多,主要与焊缝凝固速率大,偏析程度减轻,组织细化,对浸蚀液敏感性较弱以及焊缝中铁素体含量增多有关。

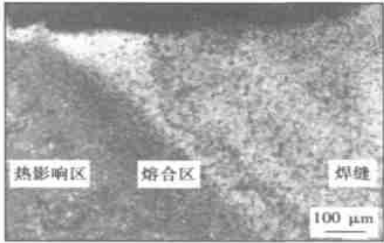


图 2 焊件预热 $200\text{ }^{\circ}\text{C}$ 时接头形貌

Fig. 2 Appearance of welded joint at $200\text{ }^{\circ}\text{C}$ of preheat temperature

2.1.1 焊缝组织形态

应用微合金化铸铁同质焊条焊接 HT250 板材,可以获得完全无白口的焊缝组织。图 3 为不同预热温度下所获得的焊缝组织。其中,图 3a 为预热温度 $T_0=0\text{ }^{\circ}\text{C}$ 时的焊缝组织,主要由珠光体、极少量铁素体和枝晶间点状石墨组成。铁素体体积分数约为 0.94% 。焊缝中初生奥氏体枝晶清晰可见,呈分枝

发达的柱状晶形态。图 3b 为 $T_0=125\text{ }^{\circ}\text{C}$ 时的焊缝组织,由珠光体、少量铁素体和细小的菊花状石墨组成及少量粗大石墨片组成。图 3c 为 $T_0=200\text{ }^{\circ}\text{C}$ 时的焊缝组织,由珠光体、铁素体和片状石墨组成,部分石墨形态呈菊花状。通过对比不同预热温度下所获得的焊缝组织可以看出,随着焊件预热温度的升高,焊缝金属的石墨化能力增强,焊缝中石墨和铁素体数量增多。焊缝中石墨主流形态由细小的点状→菊花状→片状石墨过渡。预热温度升至 $200\text{ }^{\circ}\text{C}$ 时,石墨形态已转变为细片状石墨和菊花状石墨共存。图 4 为焊缝中铁素体含量随预热温度的变化。可以看出,当 $T_0=200\text{ }^{\circ}\text{C}$ 时焊缝铁素体含量达到了 23.66% 。

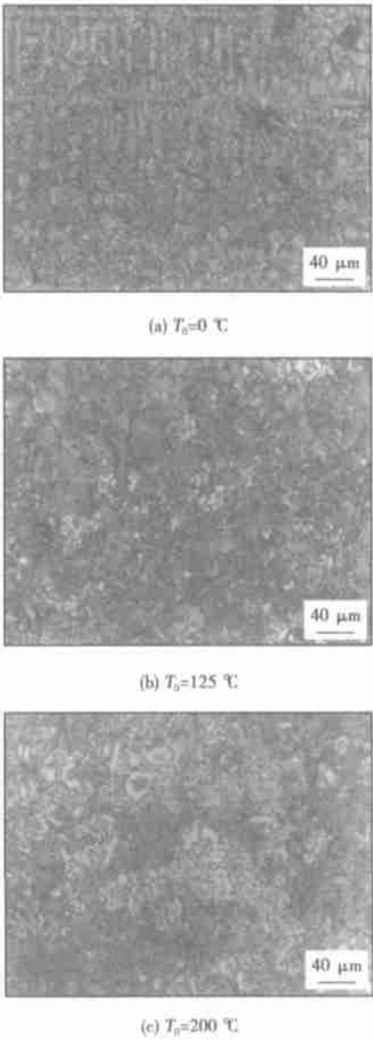


图 3 焊缝组织随预热温度的变化
Fig 3 Microstructure of weld vs preheat temperature

2.1.2 熔合区组织

熔合区紧邻母材,冷却速率较大,白口倾向高于

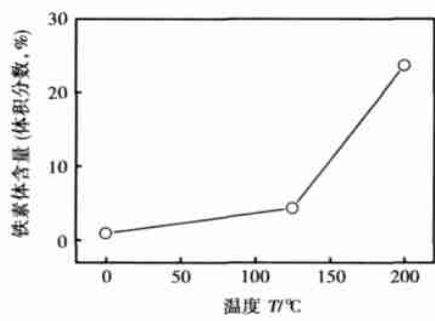


图 4 焊缝铁素体含量与预热温度的关系
Fig 4 Ferrite volume fraction vs preheat temperature

焊缝。因此,该区相组成和组织形态对预热温度更为敏感。焊件不预热焊接得到的熔合区组织由细小点状石墨、珠光体和少量自由渗碳体组成。当焊件预热到 $T_0=125\text{ }^{\circ}\text{C}$ 时,熔合区组织则由细小点状石墨、珠光体和极少量自由渗碳体组成。而当 $T_0=200\text{ }^{\circ}\text{C}$ 时,熔合区组织由少量碎块状铁素体、珠光体和过冷石墨片组成,无自由渗碳体析出,如图 5 所示。这说明,随着预热温度的升高,自由渗碳体数量显著减少,容易获得高质量的焊接接头。另外,从图 5 还可以看出,与熔合区紧邻的热影响区组织由珠光体和粗大片状石墨组成,没有产生马氏体、贝氏体和索氏体等组织。

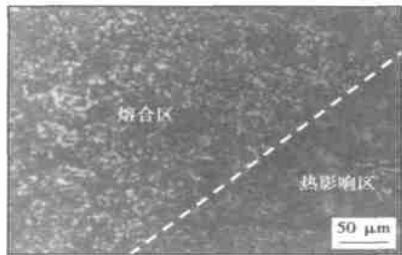


图 5 $T_0=200\text{ }^{\circ}\text{C}$ 时的熔合区组织
Fig 5 Microstructure of fusion zone at $T_0=200\text{ }^{\circ}\text{C}$

2.2 分析与讨论

2.2.1 焊接工艺对接头组织的影响

在冷焊条件下,由于冷却速率较快,熔合区极易产生渗碳体组织。采用小电流打底工艺减小了母材的熔深,使半熔化区宽度减小,从而减小了熔合区的白口宽度。焊件预热至 $T_0=200\text{ }^{\circ}\text{C}$ 时得到的接头组织见图 5,熔合区宽度只有 $245\text{ }\mu\text{m}$,且无白口组织。由此可见,小电流打底工艺对减小熔合区宽度是非常有效的。大电流连续焊工艺则增大了焊接过程的

热输入,使焊缝的冷却速度减慢,在冷却过程中有较多的时间析出石墨,有利于石墨的形核与生长,石墨析出量的增加,避免了渗碳体的产生。大电流连续焊工艺较高的焊接热输入同样减小了半熔化区的冷却速度,半熔化区石墨的析出量也有所增加,并在很大程度上抑制了渗碳体的生成,从而有效地减小了熔合区的白口宽度。

2.2.2 预热温度对接头组织与性能的影响

预热温度对焊缝和熔合区硬度分布的影响如图 6 所示。随着焊件预热温度的升高,焊缝和熔合区的硬度都呈降低的趋势。当预热温度 $T_0=200\text{ }^{\circ}\text{C}$ 时,焊缝和熔合区硬度均达到最小值,分别为 176 HB 和 198 HB。其原因在于,焊缝和熔合区组织随焊件预热温度的升高发生了显著的变化。当 $T_0=0\text{ }^{\circ}\text{C}$ 时,焊缝冷却速率较大,远远偏离平衡凝固,形成了较多的柱状晶组织。同时,细晶强化作用增强,因而焊缝硬度较高。随着预热温度的升高,焊缝和熔合区的冷却速率减小,焊缝石墨化能力显著提高,石墨生长环境得到改善,分枝趋于发达。石墨形态由最初的细小点状逐渐向菊花状、片状过渡。同时,焊缝中的石墨和铁素体含量也随着预热温度的升高而增多,珠光体含量则相对有所减少。当 $T_0=200\text{ }^{\circ}\text{C}$ 时,焊缝中铁素体的体积分数高达 23.66%,焊缝硬度大大降低。另外,熔合区析出的自由渗碳体数量逐渐减少,至 $T_0=200\text{ }^{\circ}\text{C}$ 时熔合区自由渗碳体含量为 0,且出现了少量的铁素体,从而导致熔合区硬度的降低。

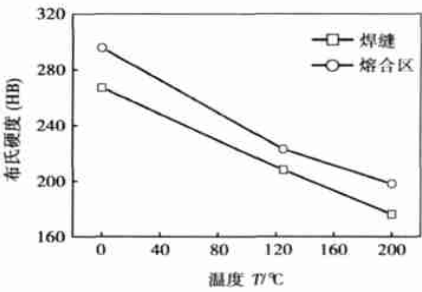


图 6 预热温度对焊补区硬度的影响
Fig. 6 Hardness of repair welding zone vs preheat temperature

从图 6 还可以看出,熔合区硬度总是高于焊缝硬度,这说明在相同预热温度下,熔合区冷却速度比焊缝冷却速度要大。熔合区与焊缝相比,珠光体含量较多,石墨化能力始终低于焊缝。由此可看出,改

善焊接接头的力学性能主要在于降低熔合区的硬度, $T_0=200\text{ }^{\circ}\text{C}$ 条件下熔合区的硬度为 198 HB, 完全可满足机械加工的要求。

2.2.3 合金成分对接头组织与性能的影响

微合金化铸铁焊芯中 C, Si 元素含量较高, 并且复合加入了 Ca, Ni, Ti, Bi 等多种石墨化元素, 焊件预热 $200\text{ }^{\circ}\text{C}$ 时焊缝的化学成分见表 2。焊芯中高的含 Si 量及适量的 Ni 元素显著提高了 Fe-C 稳定系合金的共晶温度, 使铁液在较宽的温差范围内进行石墨与奥氏体的共晶转变; Ca 与灰铁中的 S 和焊接冶金过程中渗入的 O 形成的高熔点 CaS 和 CaO 可作为石墨结晶的异质核心; Bi 与灰铁中微量的稀土元素形成的高熔点化合物也起到异质形核的作用, 都促进了熔池凝固过程中的石墨化进程; 而 Ti 元素在促成石墨化的同时对焊缝组织还起到细化作用。微量石墨化元素多元复合加入, 大大增强了焊缝的石墨化能力。焊缝金属抗拉强度达到 451 MPa, 可满足几乎所有牌号灰铸铁件的焊接修复要求。同时, 熔池中的 C, Si 元素及 Ca, Ni, Ti, Bi 等微量石墨化元素亦会向半熔化区作一定程度的扩散, 从而提高了半熔化区的石墨化能力。而传统灰铸铁同质焊条 Z248 在热态焊(预热到 $650\sim700\text{ }^{\circ}\text{C}$)条件下才可有效抑制白口组织的形成, 形成与母材性能、颜色匹配性良好的同质焊缝^[3]。由此可知, 提高焊件的预热温度只是在一定程度上抑制了白口组织的形成, 微合金化铸铁同质焊条焊接效果良好的主要原因在于焊芯中 C, Si 元素含量较高及 Ca, Ni, Ti, Bi 等多种石墨化元素的复合加入。

表 2 焊缝的化学成分(质量分数, %)

Table 2 Chemical composition of weld

C	Si	Mn	P	S	Ni	Ti	Bi	Fe
3.39	2.91	0.47	0.047	0.046	0.39	0.037	0.018	余量

3 结 论

- (1) 应用微合金化同质铸铁焊条, 采用小电流打底、大电流连续焊工艺, 对铸铁件进行焊接修复, 在预热温度低于 $200\text{ }^{\circ}\text{C}$ 条件下施焊, 即可获得组织和性能优异的同质焊缝。
- (2) 随着焊件预热温度的升高, 焊缝中石墨形态由细小的点状逐渐向菊花状及片状过渡。预热温度升至 $200\text{ }^{\circ}\text{C}$ 时, 焊缝组织由珠光体、铁素体、菊花状片墨和细片状石墨组成, 熔合区组织主要由少量碎块状铁素体、珠光体和过冷石墨片组成。
- (3) 随着焊件预热温度的升高, 焊缝金属的石墨化能力增强, 组织中石墨和铁素体数量增多, 焊缝和熔合区硬度减小。 $T_0=200\text{ }^{\circ}\text{C}$ 时得到的焊缝硬度为 176 HB, 熔合区硬度为 198 HB, 焊缝力学性能良好, 熔敷金属抗拉强度为 451 MPa, 基本上可满足各种牌号灰铸铁的焊接要求。

参考文献:

[1] 李亚江, 张永喜, 王 娟. 焊接修复技术[M]. 北京: 化学工业出版社, 2005.

[2] 孔海旺, 刘兰平. 铸铁焊接性能与工艺的分析讨论[J]. 铸造设备研究, 2001(5): 28—31.

[3] 徐锦锋, 翟秋亚, 袁 森, 等. Ca—Ni—Ti—Bi 多元微合金化铸铁电弧冷焊同质焊条的研究[J]. 西安理工大学学报, 1996, 12(4): 299—302.

[4] 翟秋亚, 徐锦锋. 多元微合金化铸铁电弧冷焊同质焊条的焊接性能[J]. 西安理工大学学报, 2000 16(4): 391—394.

[5] 周振丰. 铸铁焊接冶金及工艺[M]. 北京: 机械工业出版社, 2001.

作者简介: 翟秋亚, 女, 1963 年出生, 副教授。主要从事先进材料及其焊接方面的研究。发表论文 40 余篇。

Email: qiyazhai@xaut.edu.cn

high-temperature tensile test; endurant tensile test

Welding process of micro-alloying cast iron electrode ZHAI Qiuya, ZHAI Bo, TANG Zhen, XU Jinfeng (School of Materials Science and Engineering, Xi'an University of Technology, Xi'an 710048, China). p53—56

Abstract: Using a micro-alloying cast iron electrode the relationship between preheat temperature and microstructure and properties of joint were investigated by backing welding with low-current and then continuous welding with high-current. The results showed that the micro-alloying cast iron electrode has strong graphitizing ability and the weld metal had a little chilling tendency. The applied welding process can effectively decrease the depth of fusion zone and suppress the precipitation of cementite in fusion zone at a great extent. Thus the welding with the micro-alloying cast iron electrode can be realized at ambient temperature. When the preheated temperature is less than 200 °C, the homogeneous weld can be obtained which has the same microstructure and properties as base metal. With the increase of the preheat temperature, the graphite morphology in weld changes from spotted graphite to rosette graphite to flake graphite. The contents of graphite and ferrite increase while the hardness of the weld decreases. If the preheated temperature reaches to 200 °C, the microstructure of the weld consists of pearlite, ferrite, flake graphite and rosette graphite, and the microstructure of fusion zone consists of pearlite, small shiver ferrite and undercooled graphite. The welded joint has excellent mechanical properties.

Key words: micro-alloying cast iron electrode; iron casting; ambient temperature welding; microstructure and properties of joint

Analysis of characteristic of vertical position laser welding for aluminum alloys MIAO Yugang, CHEN Yanbin, LI Lijun, WU Lin (State Key Laboratory of Advanced Welding Production Technology, Harbin Institute of Technology, Harbin 150001, China). p57—60

Abstract: The experiments of vertical and flat position laser welding for 4 mm-thick 5A06 aluminum alloys were implemented, and the characteristics of weld dimension and porosity in the vertical position laser welding for aluminum alloys were investigated. The results show that the concave value and excessive penetration value of vertical welding is less than those of flat welding. Further, with the increase of heat input, the difference of vertical and flat welding becomes obvious. The weld appearance and dimension of the vertical welding and flat welding were slightly different. When the heat input is increased to a great extent, the weld depth of vertical welding is more than that of flat welding. However, the weld width of vertical welding is less than that of flat welding. The porosity of vertical position laser welding for aluminum alloys is composed of the large and irregular porosity or hole. It is not obviously different during vertical welding and flat welding, and a great deal of porosity concentrates in the upper and middle part of weld section, which can be indicated from the distributing position and shape of porosity. The number of porosity in vertical welding was slightly less than that of flat welding for the same welding parameters.

Key words: aluminum alloys; vertical position laser welding; flat welding; characteristic

Effect of aluminizing and diffusion treatment on adhesive strength of arc sprayed coatings WANG Qiang, LAN Dongyun, XUAN Zhaozhi, LIU Chenghui (College of Materials Science and Engineering, Jilin University, Changchun 130025, China). p61—64

Abstract: Corrosion-resisting and heat-resisting coatings of 18-8 stainless steel were made by arc spraying, aluminizing and diffusion treatment on cast iron. The microstructures and chemical compositions of coatings with aluminizing and diffusion treatment were studied by optical microscope, scanning electron microscope and X-ray diffraction. And the adhesive strength of coatings was evaluated by thermal fatigue tests. The results show that there are some regions with metallurgy bonding on the interface between coatings and substrates through aluminizing and diffusion treatment, therefore, the adhesive strength of coatings were improved greatly. And a long period of aluminizing time is adverse to the adhesive strength of coatings, so aluminizing time should be controlled well.

Key words: arc spraying; aluminizing; diffusion; adhesive strength

Microstructure and melting property of Sn-2.5Ag-0.7Cu-XGe solder MENG Gongge¹, YANG Tuoyu², CHEN Leida¹ (1. School of Material Science & Engineering, Harbin University of Science and Technology, Harbin 150040, China; 2. Anhui Science and Technology University, Bengbu 233100, Anhui, China). p65—68

Abstract: The 3 composition Sn-2.5Ag-0.7Cu-XGe lead-free solders were studied by scanning electron microscope and differential scanning calorimetry equipments. The result indicates that the microstructure is cobblestone-like pro-eutectic grain and scattered long narrow piece and small pellet eutectic mixture. With 0.5% or 1.0% element Ge, the microstructure morphology does not change. But the intermetallic compounds of Ag₃Sn and Cu₆Sn₅ tend to be fine, and their dispersion tends to be well-distributed, and Ag₃Sn phase tends to be fine needle from long narrow piece. By adding element Ge, the temperatures of the melting beginning, the melting peak and the melting finish all reduce correspondingly. And in the melting curve, the endothermic peak changes is narrow, and the melting finish part is long, but the melting temperature zone varies a little.

Key words: lead-free solder; microstructure; melting property

Solidification cracking mechanism of 690 nickel-based alloy surfacing metal BO Chunyu, YANG Yuting, CHOU Shuguo, ZHOU Shifeng (Harbin Welding Institute, China Academy of Machinery Science and Technology, Harbin 150080, China). p69—72

Abstract: Transverse restraint test was used to investigate the solidification cracking mechanism of 690 nickel-based alloy surfacing metal. Results show that the solidification cracking susceptibility of 690 nickel-based alloy surfacing metal is closely correlated with the segregation process during welding, which is greatly influenced by Nb. The solidification temperature of 690 nickel-based alloy surfacing metal falls when the Ni, Nb-rich phases segregate on the grain boundary or subgrain boundary, which induces that the ductility decreases and the appearance is fined. Then, cracking initiates and